JOURNAL OF AIRCRAFT
Vol. 37, No. 1, January–February 2000

Experiments on a 60-Degree Delta Wing with Rounded Leading-Edge Vortex Flaps

Kenichi Rinoie*
Cranfield University, Bedford, England MK43 0AL, United Kingdom

Low-speed wind-tunnel measurements were done on a 1.15-m span 60-deg delta wing with rounded leading-edge vortex flaps. The purpose of the measurements is to assess the benefits of the rounded leading-edge vortex flaps in regard to improving the lift/drag ratio of delta wings. Force and surface pressure measurements were made at a Reynolds number based on a centerline chord of 2×10^6. The increase in the radius of the rounded leading edge reduces the drag significantly both with and without flap deflection except in the minimum drag region. Deflecting the rounded leading-edge vortex flap improves the lift/drag ratio at relatively higher lift coefficients, when compared with the sharp-edged vortex flap. The largest improvement in the lift/drag ratio as compared with the sharp-edged delta wing with vortex flaps is more than 25% in the lift coefficient range between about 0.6 and 0.8 for the rounded-edge delta wing with flaps that were deflected 30 deg downward.

Nomenclature

b	= local span, m
C_A	= axial force coefficient
C_A/C_{Aell}	= attainable thrust ratio
C_D	= drag coefficient
C_L	= lift coefficient
C_m	= pitching moment coefficient nondimensionalized using Cr and measured about $x/Cr = 0.4$
Cp	= pressure coefficient
Cr	= wing centerline chord, m
D	= rounded leading-edge diameter, m
L/D	= lift/drag ratio
U_∞	= freestream velocity, m/s
x	= chordwise coordinate measured from the apex of the delta wing, m
y	= spanwise coordinate orthogonal to x, measured from the wing centerline, m
α	= wing angle of attack, deg
δ_f	= vortex flap deflection angle measured normal to the hinge line for an original wing without leading-edge modification, deg
δ_{fc}	= corrected vortex flap deflection angle for a wing with leading-edge modification, deg

Notation

$/n$	$= \delta_f = n (n = 0°–60°)$

Introduction

A LEADING-EDGE vortex flap (LEVF) improves the low-speed aerodynamic characteristics of a delta wing.[1] A pair of leading-edge separation vortices, which are formed over the sharp-edged delta wing, produces an upward suction force that increases the drag component and consequently decreases the lift/drag ratio (Fig. 1a). The LEVF is a leading-edge deflectable surface. When the LEVF is deflected downward, a leading-edge separation vortex is formed over the forward-facing surface. The suction force produced by this vortex may reduce the drag component and increase the lift/drag ratio, which plays an important part in improving the takeoff and climb performance of delta wing aircraft (Fig. 1b). Many studies using different flap configurations have confirmed the benefit of the LEVF.[2–9] The camber line of the delta wing changes due to the flap deflection. This partly explains the reason for aerodynamic benefits of the LEVF.

Another way to improve delta wing performance is to use a rounded leading edge. A large fraction of the leading-edge suction force will act on the rounded leading edge and so reduce the drag component of the delta wing (Fig. 1c). Numerous studies have been done to investigate the effects of the rounded leading edge.[10–13] They confirmed the benefit of the rounded leading edge, but pointed out the dominance of the effect of the Reynolds number on the performance of a rounded-edged wing. Note that there are drawbacks of the rounded leading edge compared with the sharp leading edge, that is, first, reduction in lifting performance as vortex lifts are efficiently traded for thrust and, second, increase in the wave drag component at supersonic flight.

These studies on the rounded leading-edge delta wings have led to the idea that a combination of LEVF and the rounded leading edge might greatly improve the characteristics of the LEVF. By deflecting the rounded leading-edge LEVF, suction forces that are caused both by the leading-edge separation vortex over the flap surface and by the rounded leading edge may reduce the drag component and increase the lift/drag ratio (Fig.1d). A previous study on the LEVF[1] by Rao investigated a delta wing with rounded leading edges. Sharp-edged thin plates were attached to the original rounded-edge delta wing as the LEVF. The reported L/D improvements in Ref. 1 were caused by the sharp leading-edge vortex flaps, as in Refs. 2–9.

Some preliminary wind tunnel tests[14,15] were conducted at Cranfield University to study the rounded-edge vortex flap. A 60-deg rounded leading-edge delta wing model with an airfoil section with a thickness of 10% was tested at a Reynolds number that was based on a centerline chord of 8×10^5. Although the tests were done at a relatively low Reynolds number, the results indicated positive aspects of the rounded leading-edge delta wing with a deflected LEVF as compared to a sharp-edged flat delta wing. These results encouraged the present author to conduct further wind-tunnel tests to confirm the benefits of rounded LEVF. Differences in the vortex flap deflection angle and in the radius of the rounded leading edge will affect the performance of the delta wing.

Tests were conducted in a Cranfield University 2.4×1.8 m low-speed wind tunnel. The 60-deg delta wing model[5] was again used by modifying the originally sharp leading edge into a rounded one. The force and surface pressure measurements were made on this delta wing model with different LEVF deflection angles and with three different rounded leading edges. Measurements were made

Presented as Paper 98-3.6.1 at the 21st International Council of the Aeronautical Science Congress (ICAS), Melbourne, Australia, 13–18 September 1998; received 28 February 1999; revision received 14 May 1999; accepted for publication 21 May 1999.

*Visiting Research Fellow, College of Aeronautics; currently Associate Professor, Department of Aeronautics and Astronautics, University of Tokyo, 7-3-1 Hongo, Bunkyo-ku, Tokyo 113-8656, Japan. Member AIAA.

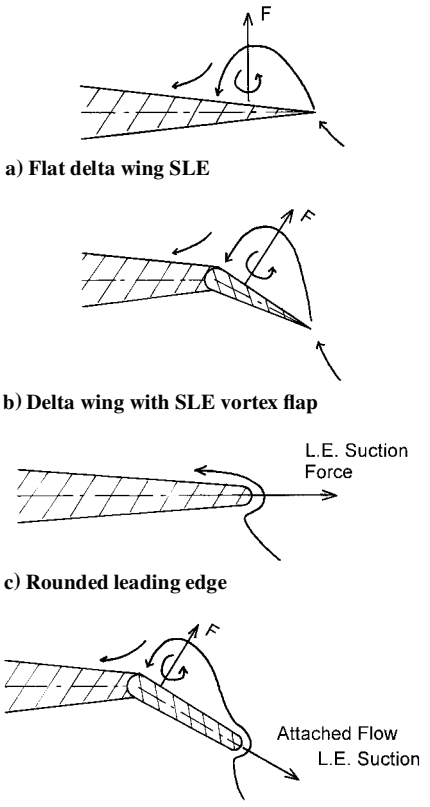

Fig. 1 Concept of vortex flap and rounded leading edge.

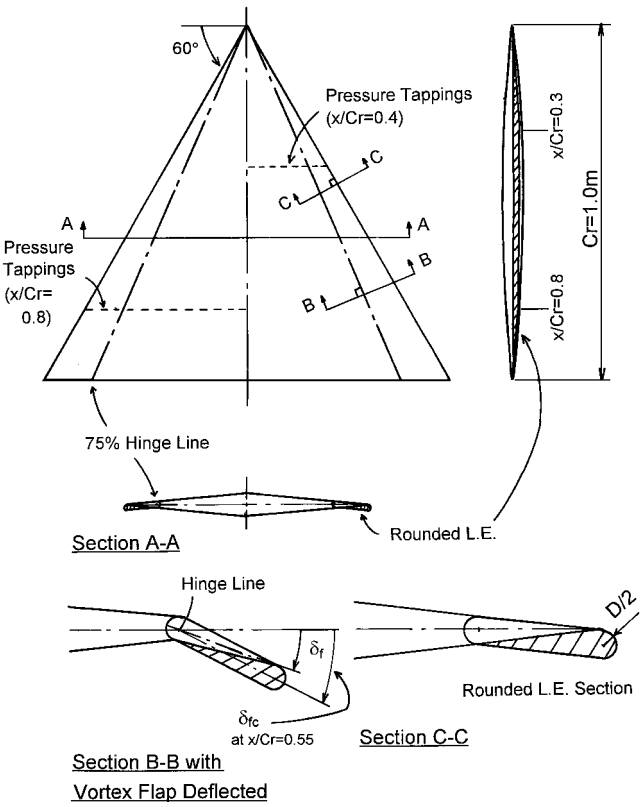

Fig. 2 Delta wing model with rounded leading-edge LEVF.

in a range of angles of attack from −4 to +36 deg at a Reynolds number based on the wing centerline chord of 2×10^6.

In summary, the purpose of this study is to confirm the benefits of rounded leading-edge vortex flaps, to study the effects of the difference in the rounded leading-edge radius on wing performance, and to investigate the optimum vortex flap deflection angle that gives the maximum lift/drag ratio.

Experimental Details

Figure 2 shows the model details. It is the same one that was tested in Ref. 5, except for the leading-edge modification. The original model is a sharp-edged 60-deg delta wing with a centerline chord length Cr of 1 m. It has a symmetrical convex airfoil section with a maximum thickness/chord ratio of 4.8%. The spanwise thickness distribution varies linearly from the centerline to the tip. The details of this original wing section are described in Ref. 5. Two rows of pressure tappings are located on the upper surface. The model has the LEVF hinge lines running from the wing apex to 75% of the trailing-edge semispan station. Flap deflection angle δ_f is defined as the angle between the mean line of the original wing and that of the vortex flap without leading-edge modification, measured in the plane that is normal to the hinge line (see section B-B in Fig. 2). Nine different flap deflections of $\delta_f = 0$, 10, 15, 20, 25, 30, 40, 50, and 60 deg were tested.

Rounded leading-edge modifications were made by attaching rounded leading-edge sections to the lower surface of the original wing (Fig. 3). The plan shape of this section is the same as that of the vortex flap, so that the latter can be deflected. It has a constant leading-edge diameter D between the chordwise stations of $x/Cr = 0.3$ and 0.8. The diameter is defined in the plane that is normal to the leading-edge line (see section C-C in Fig. 2). This diameter decreases linearly to zero from $x/Cr = 0.3$ toward the apex and from $x/Cr = 0.8$ toward the trailing edge. The thickness of this section in a spanwise direction also decreases to zero toward the flap hinge line. Three different leading-edge diameters ($D = 5$, 15, and 30 mm) were tested. The ratio of the rounded leading-edge radius to the root chord length is 0.25, 0.75, and 1.5% for $D = 5$, 15, and

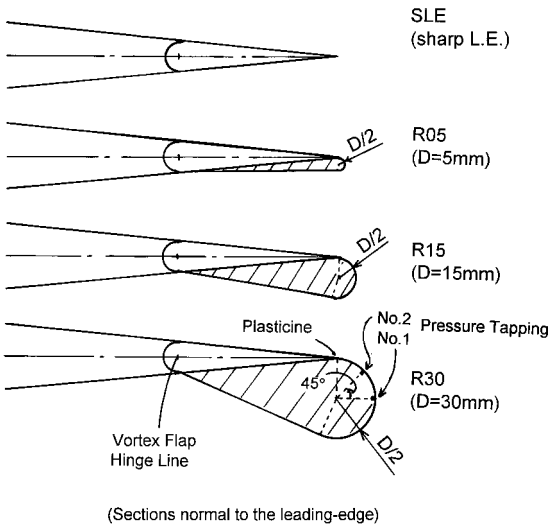

Fig. 3 Different rounded leading-edges.

30 mm, respectively. The increase in the wing area when $\delta_f = 0$ deg that is caused by the attached rounded-edge sections is 0.75, 2.25, and 4.5% for $D = 5$, 15, and 30 mm, respectively. Two pressure tappings are located on the $D = 15$ and 30 mm rounded leading-edge sections (Fig. 3). The chordwise positions of the pressure tappings are the same as those of the main wing. Any irregularities along the intersection between the original wing and the rounded-edge section were carefully blended by using Plasticine.

The experiments were made in a Cranfield University 2.4×1.8 m low-speed, closed working section, closed-return wind tunnel. Most of the tests were made at a tunnel speed of $U_\infty = 30$ m/s. The Reynolds number based on the wing centerline chord was 2×10^6 when $U_\infty = 30$ m/s. The freestream turbulence intensity of the tunnel is about 0.09%. The model was mounted, inverted from the overhead balance, by a single shielded strut and a tail wire at the

centerline of the tunnel. The angle of attack was in a range from −4 to +36 deg. Lift, drag, and pitching moment were measured using an overhead six-component electro–mechanical balance. The aerodynamic coefficients were obtained using the same tunnel boundary correction methods that were used in Ref. 5. Although the main wing area increased because of the attached rounded-edge sections, all of the aerodynamic coefficients were calculated based on the original sharp-edged delta wing area when $\delta_f = 0$ deg. The estimated overall accuracy of the coefficients is better than ±2% at 20:1 odds. Although tunnel boundary corrections were applied, accuracy at higher angles of attack is believed to decrease because of the higher tunnel wall interference. Surface pressure distributions were measured using a scanivalve that was mounted within the model. The estimated overall accuracy of the pressure coefficient is ±3% at 20:1 odds. Surface pressure measurements were made for the models with rounded edges that were $D = 15$ and 30 mm.

The effects of the Reynolds number that are dominant for the rounded-edgedelta wing, as noted in Refs.10–13, are also important in the performance of the rounded-edge vortex flap. Therefore, supplementary tests were made to examine the effect of the Reynolds number by increasing wind-tunnel speed to $U_\infty = 45$ m/s and by adding roughness strips to the leading edge of the model. It was expected that the drag coefficient decreases as the Reynolds number increases. However, changes in aerodynamic coefficients of the present experiment were too small to confirm the effects of Reynolds number.

Examples of the notation used in this paper are as follows. The sharp leading-edge (SLE) wing without any flap deflection ($\delta_f = 0$ deg) is SLE/00, and the rounded leading edge $D = 5$ mm with a flap deflection of $\delta_f = 30$ deg is R05/30.

Experimental Results

Prior to these measurements three component force measurements for the original sharp-edged wing with $\delta_f = 0$ and 30 deg were repeated and compared with data from Ref. 5 for the same wing configurations. The present data agree with those from Ref. 5.

Three-Component Balance Measurements

Figures 4a–4g show the lift, drag, lift/drag, and pitching moment curves for three different rounded-edge models with and without flap deflection ($\delta_f = 0$ and 30 deg) together with the results from the sharp-edged wing. The C_L vs α curves in Fig. 4a show that, as the radius of the rounded edge increases, C_L decreases slightly, even though the original delta wing area is used as a reference area. Deflecting the LEVF decreases the C_L for all models, as was expected. The data for SLE/30 and R05/30 show discontinuities at about $\alpha = 18$ deg. Surface pressure measurements for SLE/30 indicated that spanwise length of the leading-edge separation vortex increases as α increases and that the angle of attack α of 18 deg almost coincides with the angle when the spanwise length of the leading-edge separation vortex becomes larger than the vortex flap span length. It is thought that this has caused the increase in the lift and resulted in the discontinuities at about $\alpha = 18$ deg in C_L vs α curves. Comparisons of the lift coefficient with 60-deg flat-plate delta wing data from Ref. 16 are also shown in Fig. 4a. In Ref. 16, measurements were made using a 60-deg, 0.10-in. thickness flat-plate delta wing with beveled sharp edges at a Reynolds number of 10^6. Although there is some scattering in the results, the slope of the lift curve agrees with these data ($\delta_f = 0$ deg, SLE/00) until about $\alpha = 25$ deg. The discrepancy in the C_L at $\alpha = 0$ deg is caused by the presence of a shielded strut in the present measurements, as was noted in Ref. 5. The discrepancy near $C_{L\max}$ can be attributed to vortex bursting, as was noted in Ref. 9.

Figure 4b shows the C_D vs α curves. Increasing the radius of the leading edge reduces C_D except in the minimum drag region. This decrease in C_D is caused despite the flat delta wing area being used as a reference area. Note that even the smallest increase in the rounded-edge radius (R05/00 and R05/30) decreases C_D. A high suction effect of the rounded leading edge is demonstrated. The C_L–α and C_D–α curves in Figs. 4a and 4b show decreases in C_L and C_D when the rounded leading-edge radius is increased. Similar results without LEVF deflection are seen in Ref. 11, where experiments were made on 60-deg flat delta wings with sharp and rounded leading edges.

Figure 4c shows the C_D vs C_L curves when $C_L < 1.0$. The significant effect of flap deflection on C_L is clearly seen in Fig. 4c. Note that the C_D is derived by using the datum flat delta wing area as reference, even when the vortex flap is deflected. When the flap is deflected, the projected planform area is reduced and so the drag coefficient will increase. Therefore, the effects of vortex flaps are difficult to evaluate from the C_L and C_D data. The L/D ratio is free from the wing reference area and so it is a good measure to evaluate the LEVF performance. In Fig. 4c, the minimum values of drag coefficients $C_{D\min}$ for each wing configuration are shown. When the flap is deflected and when the rounded leading-edge radius is increased, the value of $C_{D\min}$ increases.

Figures 4d shows L/D vs C_L when $\delta_f = 0$ and 30 deg. Comparisons with SLE/00, R15/00, and R30/00 in Fig. 4d show a limited level of improvement in the maximum L/D due to the rounded edge when $\delta_f = 0$ deg. However, at C_L values greater than 0.2, R15/00 and R30/00 show better L/D ratios than does SLE/00. Comparisons for the three models at $\delta_f = 30$ deg show no improvement in the maximum L/D due to leading-edge roundness. The maximum L/D value of R30/30 is significantly smaller than those in SLE/30 and R15/30. However, at C_L values higher than 0.5, the L/D of R30/30 shows the highest value of L/D.

To more clearly visualize the LEVF deflection effects on L/D, the percent increase in L/D for R15, R30, and SLE/30 wings as compared with the SLE/00 wing is plotted in Fig. 4e. This shows that the L/D without any flap deflection (R15/00 and R30/00) increases to more than 10% above that of the SLE/00 wing for lift coefficients greater than 0.2. The sharp-edgedLEVF wing (SLE/30) shows better performance than R15/00 and R30/00 in the C_L range between 0.2 and 0.6. The most significant L/D improvement, which is more than 50% as compared with the sharp flat delta wing, is observed for R30/30 at about $C_L = 0.6$.

It is important to compare results of R15 and R30 wings with those of SLE wing, when three wing configurations have similar camber lines, that is, at the same flap deflection angle. Therefore, the percent increase in L/D for R15/30 and R30/30 wings as compared with the SLE/30 wing is plotted in Fig. 4f. Figure 4f shows that rounded edges with LEVF (R15/30 and R30/30) improve L/D more than the SLE/30 configuration for C_L values that are greater than 0.5. The most significant L/D improvement, which is more than 25% as compared with the SLE/30, is observed for R30/30 between C_L of about 0.6 and 0.8. Strictly speaking, SLE/30, R15/30, and R30/30 have slightly different flap deflection angles. This will be explained in the next section.

Figure 4g shows the pitching moment curves vs C_L. The LEVF and rounded edge has little effect on C_m. The aerodynamic center position, which was measured using the C_m–C_L slope, is about $0.57Cr$ for all examples.

Surface Pressure Measurements

Figures 5 and 6 show surface pressure distribution for R15, R30, and SLE[5] in the spanwise direction for the upper surface at $x/Cr = 0.4$. The spanwise coordinate is normalized by the length of the original wing local semispan. The angles of attack referred to here are those measured from the tunnel centerline and have not been corrected for tunnel wall interference. To clarify the effects of rounded leading edge, pressure distributions at constant angles of attack of $\alpha = 6$, 12, and 18 deg at $x/Cr = 0.4$ are shown in Figs. 5 ($\delta_f = 0$ deg) and 6 ($\delta_f = 30$ deg). The formation of the leading-edge separation vortex is observed in most parts of Figs. 5 and 6 except in Fig. 6a. In Fig. 5a ($\alpha = 6$ deg), one can see that the suction region is present on all three wings. As the radius of the rounded edge increases, the suction peak decreases and the spanwise length of the suction region becomes shorter. A similar trend is seen at $\alpha = 12$ deg (Fig. 5b). For $\delta_f = 30$ deg and $\alpha = 6$ deg in Fig. 6a, the effects of the rounded edge are very small. However, at higher angles of attack [such as $\alpha = 12$ and 18 deg, (Figs. 6b and 6c)], an increase in the

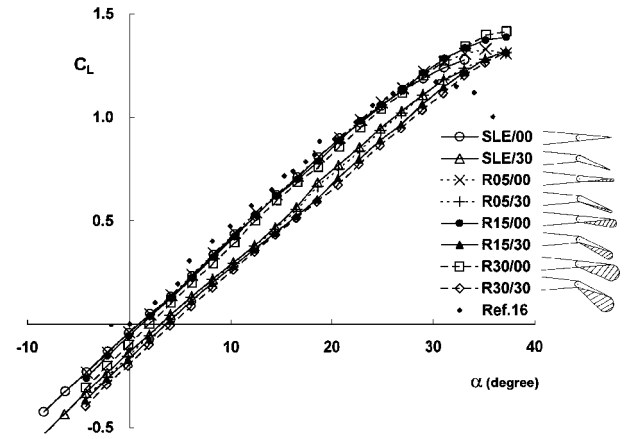

a) C_L–α

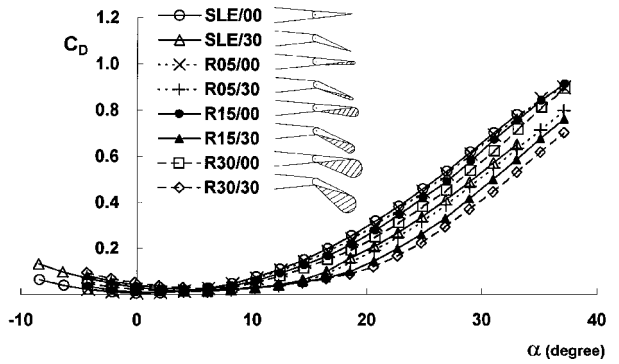

b) C_D–α

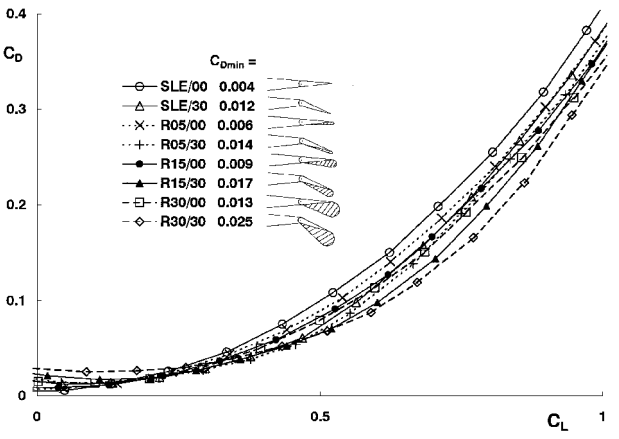

c) C_D–C_L

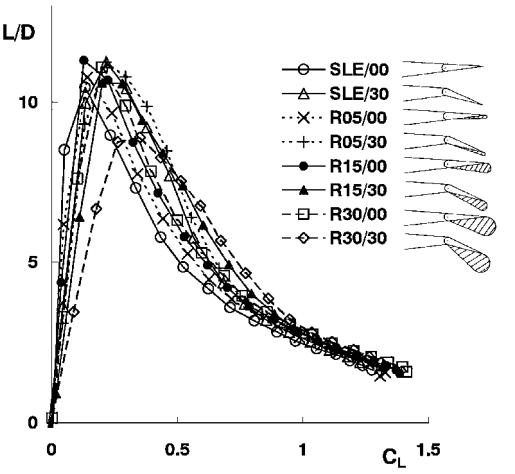

d) L/D–C_L

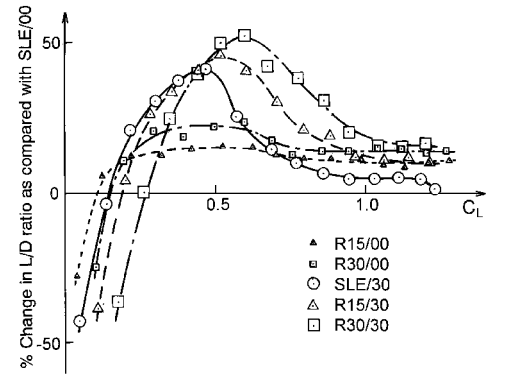

e) Percent improvement in L/D as compared with SLE/00

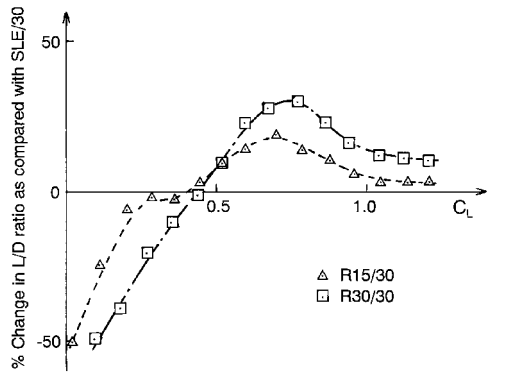

f) Percent improvement in L/D as compared with SLE/30

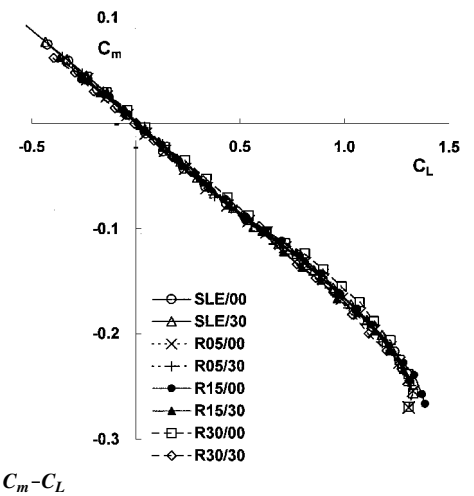

g) C_m–C_L

Fig. 4 Effects of rounded leading edge with and without flap deflection.

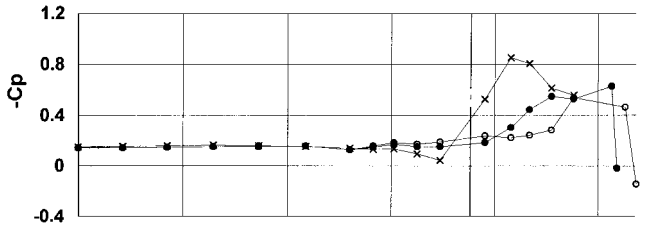

a) α = 6 deg

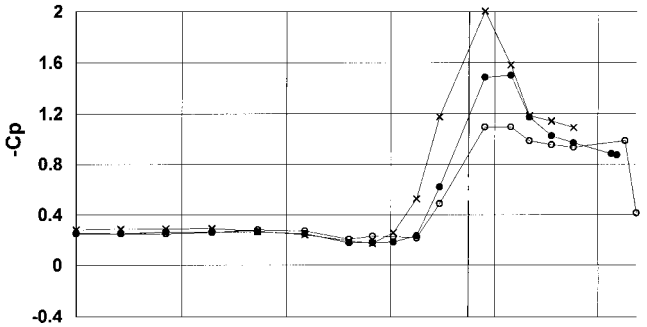

b) α = 12 deg

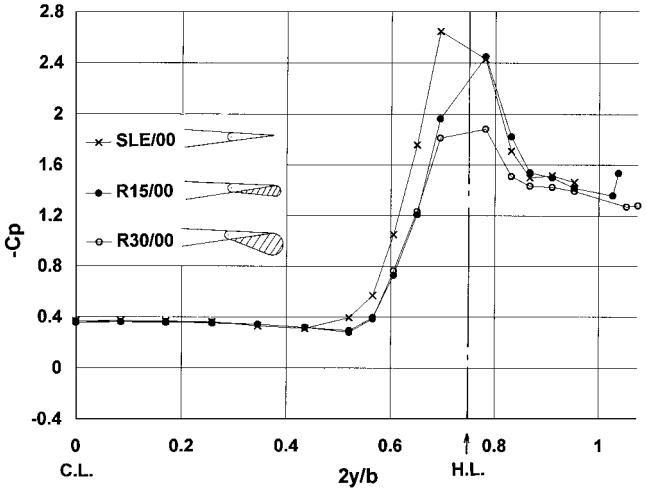

c) α = 18 deg

Fig. 5 Surface pressure distribution at constant α (δ_f = 0 deg).

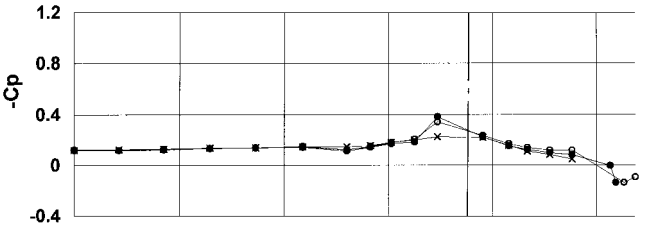

a) α = 6 deg

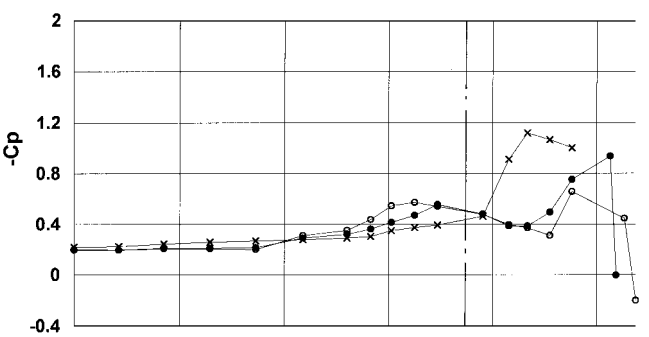

b) α = 12 deg

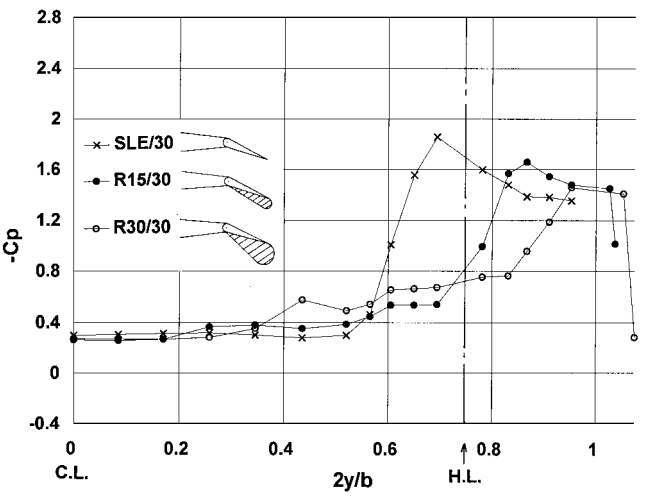

c) α = 18 deg

Fig. 6 Surface pressure distribution at constant α (δ_f = 30 deg).

rounded edge radius significantly reduces the spanwise length of the suction region as for $\delta_f = 0$ deg.

Effects of the Rounded Leading-Edge Radius on Different δ_f

Cp and *L/D* Distributions

To examine the effects of flap deflection, force and surface pressure measurements were made for nine different flap deflection angles. Figure 7 shows examples of these measurements. Surface pressure distributions for the R15 wing at a constant angle of attack α of 12 deg for nine different δ_f at $x/Cr = 0.4$ are shown. As the vortex flap is deflected, the suction region that is over the surface of the flap shrinks, and the suction region that is inboard of the flap hinge line becomes larger. Therefore, it appears that increasing δ_f precipitates flow separation from the flap hinge line, causing a vortex inboard of the hinge line while simultaneously suppressing separation from the flap surface. These tendencies are the same as those in a previous study using an SLE.[5] The suction pressure near the leading edge decreases as the flap is deflected downward.

Comparisons of the three types of wings were done at a constant lift coefficient, to show the effects of flap deflection more clearly. Figure 8 shows the L/D vs flap deflection angle at a constant C_L of 0.25 (Fig. 8a) and 0.5 (Fig. 8b). The data were obtained from

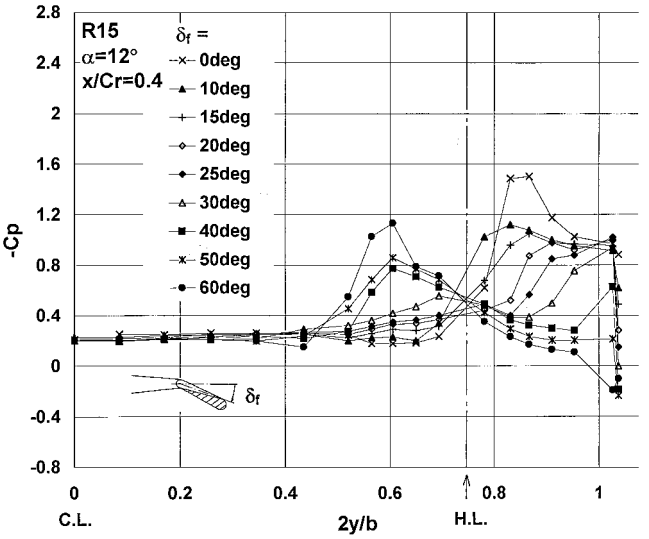

Fig. 7 Surface pressure distribution at different δ_f (R15, α = 12 deg).

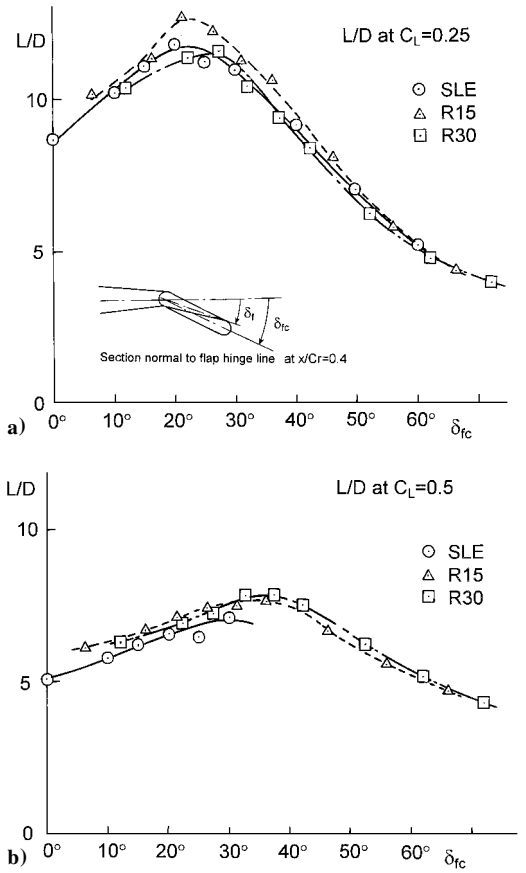

Fig. 8 ***L/D*** **vs corrected** δ_f **at constant** C_L**.**

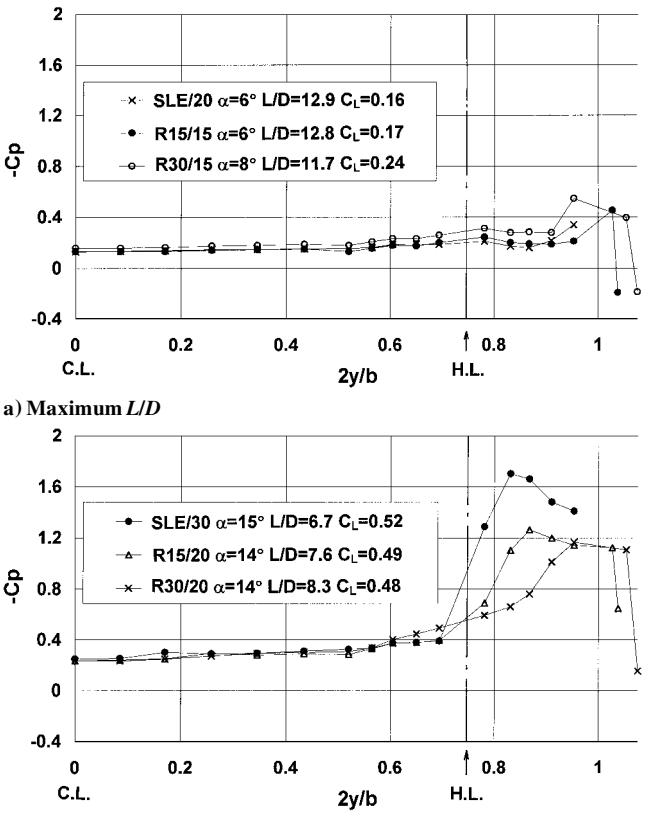

Fig. 9 Surface pressure distribution for optimum ***L/D*** **configurations.**

L/D–C_L distribution for nine different flap deflection angles. Because the rounded leading-edge section was attached to the lower surface of the sharp-edged wing, the true flap deflection angle is greater than δ_f for the R15 and R30 wings. The δ_{fc} in Fig. 8 shows this corrected (true) flap deflection angle. Here, the true flap deflection angle at $x/Cr = 0.55$, which is a midchordwise station of the constant radius rounded leading-edge section (see Fig. 2), is defined as δ_{fc}. The corrected vortex flap deflection angle δ_{fc} at $x/Cr = 0.55$ is

$$\delta_{fc} = \delta_f + \tan^{-1}\left\{\frac{2D\sin(\varepsilon+\Lambda)}{0.55Cr\sin\Lambda}\left[1\Big/\tan\left(\frac{\pi}{2}-\Lambda\right)\right]\right\}$$

where ε is the semi-apex angle of the main wing inboard of the flap hinge line and Λ is the wing sweepback angle of 60 deg.

The L/D vs δ_{fc} curves at $C_L = 0.25$ in Fig. 8a are similar for all three wings. However, the R15 wing had larger L/D for almost the entire range of δ_{fc}. The absolute maximum L/D at $C_L = 0.25$ is about 12.7 when R15 and $\delta_{fc} = 21$ deg ($\delta_f = 15$ deg). The L/D has increased about 9% when compared with the sharp-edged delta wing at $\delta_{fc} = 20$ deg (the maximum value of L/D is 11.7 for SLE at $\delta_f = 20$ deg). Figure 8a also shows that the R30 wing is not as effective as the R15 wing. Figure 8b shows the L/D vs δ_{fc} curves at $C_L = 0.5$. The L/D vs δ_{fc} curves are similar for the R15 and R30 wings. The maximum L/D at $C_L = 0.5$ is about 7.8, which was attained for the R30 wing between $\delta_{fc} = 32.5$ and 37.5 deg ($\delta_f = 20$ and 25 deg). The percent increase in the maximum L/D as compared with that of the SLE wing is about 10% (the maximum value of L/D is 7.1 for SLE at $\delta_f = 30$ deg). The measurements for the original sharp-edged wing were made for a limited number of examples. However, because the results in Ref. 5 indicated that δ_f greater than 40 deg is not as effective as δ_f that is smaller than 30 deg, it was concluded that the maximum L/D for the sharp-edged wing at $C_L = 0.5$ was attained at $\delta_f = 30$ deg. Results in Figs. 8a and 8b mean that the rounded leading-edge vortex flaps are more effective than the sharp-edged vortex flaps at relatively high lift coefficients ($C_L \geq 0.5$).

Optimum ***L/D*** **Condition**

Figure 9a shows pressure distribution for three wings (R15, R30, and SLE[5]) when the absolute maximum L/D was attained for each wing. Here, the maximum L/D that was attained for each wing is called the absolute maximum L/D. Note that the absolute maximum L/D, which corresponds to the true peak in the L/D curve, is difficult to accurately evaluate because the true peak in the L/D curve often lies between two of the data points, as was noted in Ref. 9. Here, the observed maximum L/D configurations from Fig. 4d were used to discuss the pressure distributions. As was discussed in Ref. 5, the maximum L/D for the sharp-edged wing is attained when the flow attaches on the flap surface without forming a large separation vortex. Figure 9a shows that, for the R15 and R30 wings, only a small suction region at the leading edge is observed. Therefore, the absolute maximum L/D for the rounded-edged wing with a vortex flap is attained at flow conditions similar to those for the sharp-edged wing, when there is only a small separated region and no large separation vortex on the surface of the flap. Traub[17] discussed separately the effects of vortex flaps and the rounded leading edge. In Ref. 17, it was stated that the optimum performance of the blunt-edged wing with the LEVF would be attained when separation on the flap surface is suppressed. Present results confirm the discussion in Ref. 17. In Fig. 9a, the numerical values of the maximum L/D for each of the three wings are also shown. The maximum L/D values for each wing are 12.9 for the SLE wing at $\delta_f = 20$ deg, 12.8 for the R15 wing at $\delta_f = 15$ deg, and 11.7 for the R30 wing at $\delta_f = 15$ deg. This indicates that use of the rounded edge did not improve the maximum L/D.

Figures 4d, 4e, and 4f indicated that the benefit of rounded LEVF is seen at relatively high C_L. Therefore, it is of interest to see the flow patterns over the wing and flap surfaces when the rounded LEVF indicates the benefit at relatively high C_L. Figure 9b shows the pressure distributions when the local maximum L/D is attained at a constant C_L of 0.5 for the three wing configurations. The local maximum L/D is the maximum L/D that was chosen from the data for different α and δ_f when the measured C_L is almost equal to 0.5. This local maximum L/D configuration was determined from

Fig. 8b. Because the pressure measurements were made at a specific angle of attack without taking C_L into account, the Cp distributions when C_L is the closest to the constant value of 0.5 are shown. The Cp distributions in Fig. 9b show that a separation vortex is formed on the surface of the vortex flap for all three configurations. The spanwise length of the vortex for the SLE/30 is very similar to the length of the flap span. As the radius of the rounded leading edge increases, the suction peak of the vortex decreases. Figure 9b shows that the separation vortex is almost confined to the flap at the local maximum L/D when $C_L = 0.5$.

Axial Force Distributions

Figure 10 shows axial force coefficients C_A vs C_L curves. C_A is defined by

$$C_A = C_D \cos\alpha - C_L \sin\alpha$$

The negative value of C_A is caused not only by the leading-edge suction force but also by suction pressure acting on the positive slope area on the upper rounded surface near the leading edge. The SLE/00 wing has a small negative value of C_A at C_L values higher than 0.3. However, the suction component of C_A for the R15/00 and R30/00 wings is much larger than the SLE/00. Figure 10 also shows the results from Ref. 11. The tests in Ref. 11 were made on 60-deg flat-plate delta wings that had sharp and rounded leading edges. The models used have a maximum thickness to local chord ratio of 3%. The rounded leading-edge radius that was normalized by the local chord length is 1.582%, which is almost equivalent to the R30/00 model used in this study. Measurements were made at a Reynolds number that was based on a mean chord of 1.6×10^6. The C_A curves of Ref. 11 show similar distributions to those of present measurements for $\delta_f = 0$ deg wings. As the radius of the leading edge increases, the negative value of C_A increases at a higher C_L.

The C_A distributions for the wing with vortex flaps show that a strong suction force is acting on the wing at C_L values higher than 0.2, even for the sharp-edge wing (SLE/30). The minimum C_A in Fig. 10 is attained for the R30/30 wing. This corresponds to that the R30/30 attained the maximum L/D at C_L values higher than 0.5, as shown in Fig. 4d. It is significant that the sharp-edged wing with vortex flaps (SLE/30) achieves almost the same axial suction force as that of the rounded leading-edge flat delta wing (R30/00) at C_L higher than 0.7.

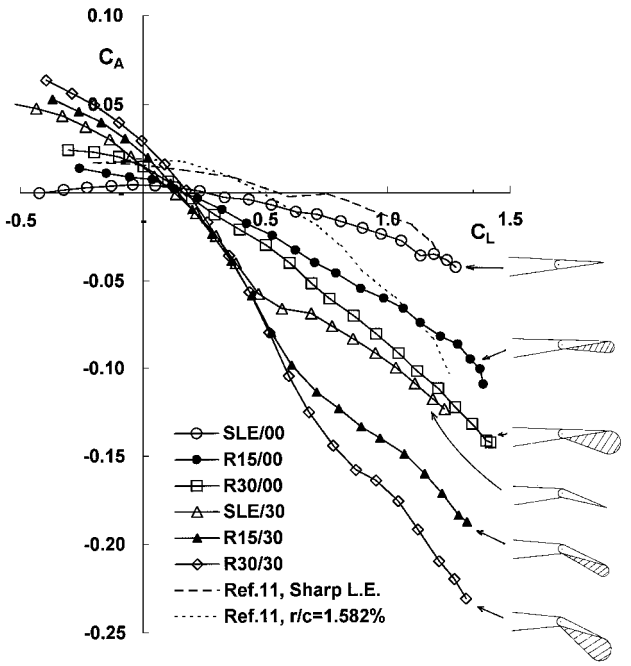

Fig. 10 Axial force C_A vs C_L.

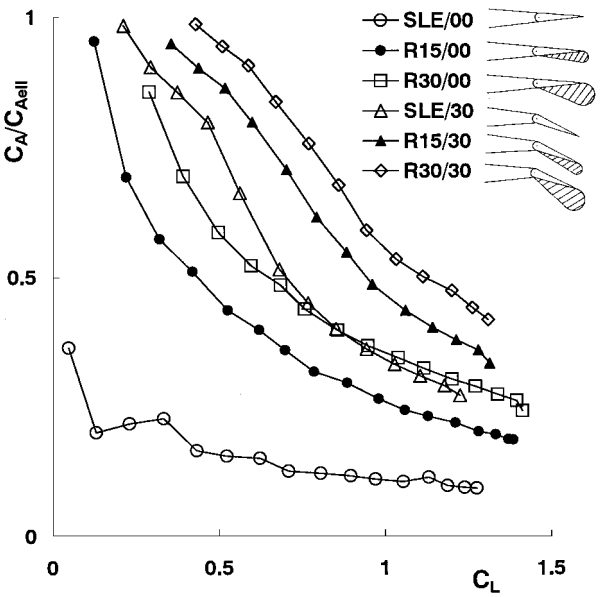

Fig. 11 Attainable thrust ratio C_A/C_{Aell} vs C_L.

Figure 11 shows the attainable thrust ratio C_A/C_{Aell} vs C_L curves. C_A/C_{Aell} is defined by

$$\frac{C_A}{C_{Aell}} = \left[\frac{(C_D - C_{D\min})\cos\alpha - C_L \sin\alpha}{(C_L^2/\pi AR)\cos\alpha - C_L \sin\alpha}\right]$$

where AR is a wing aspect ratio. This expression shows the measured axial force divided by the theoretical maximum axial force, that is, that for a wing with elliptic spanwise loading. This parameter ranges between 0 (no thrust) and 1 (full thrust). Figure 11 shows that the attainable thrust ratio increases as flap deflection angle is increased and as the radius of the rounded leading edge is increased. As C_L increases, C_A/C_{Aell} decreases for all configurations. Except for SLE/00, almost full thrust is observed when C_L is relatively small. These results indicate abilities to recover suction both for vortex flaps and rounded leading edges. The results for sharp-edged wing in Fig. 11 are similar to those reported in Ref. 7 for double delta wing with vortex flaps.

According to these results, the benefit of the rounded leading edge can be clearly seen at relatively high lift coefficients (C_L greater than 0.5). The surface pressure measurements in Figs. 5, 6, and 9b indicated that the spanwise length of the suction region that was formed on the surface of the flap was reduced and that the suction peak decreased as the radius of the rounded edge increased. However, Figs. 4e and 4f indicated that the L/D is improved as the radius of the leading edge is increased at relatively high C_L. These two facts suggest that the leading-edge suction force acting on the rounded leading-edge might have helped to improve the L/D ratio. In Ref. 18, it was indicated that the leading-edge suction force caused by the rounded leading edge is highly dependent on the formation of the leading-edge separation vortex and the wing configurations. Further study is necessary to reveal the effect of the rounded leading edge.

In this study, the benefits of a rounded leading-edge vortex flap at low speed were investigated. Research on rounded leading-edge vortex flaps at supersonic speeds is an important topic because delta wing aircraft often fly at supersonic speeds.

Conclusions

Force and surface pressure measurements were made using a 1.15-m span 60-deg delta wing model at the Reynolds number of 2×10^6 that was based on the centerline chord to investigate the effects of a rounded leading edge with and without vortex flaps.

1) The increase in the radius of the rounded leading edge reduces the drag significantly both with and without flap deflection except in

the minimum drag region. The increase in the radius of the rounded leading edge reduces the spanwise length of the suction pressure region on the surface of the flap.

2) A rounded leading-edge delta wing without any vortex flap deflection affords approximately a 10% improvement in lift/drag ratio relative to the sharp-edged flat delta wing at lift coefficients greater than 0.2.

3) Deflecting the rounded leading-edge vortex flap improves the lift/drag ratio as compared with the sharp-edged vortex flap at relatively high lift coefficients (C_L values greater than 0.5). The greatest percentage improvement in the lift/drag ratio as compared with the sharp-edged delta wing with vortex flaps is more than 25% in the lift coefficient range between about 0.6 and 0.8 for a 30-deg flap deflection angle with a 30-mm-diam rounded leading-edge vortex flap.

4) The absolute maximum lift/drag ratio for the rounded edge wing with the vortex flap deflection is achieved when there is no large area of separation over the deflected vortex flap surface; this agrees with the observations made for the sharp-edged delta wing. However, the absolute maximum lift/drag ratio for the rounded-edge wing was not improved when compared with the sharp-edged wing.

Acknowledgments

The author expresses his gratitude to J. L. Stollery, College of Aeronautics, for his beneficial advice. He also expresses his gratitude to members of the workshop in the College of Aeronautics for their help in performing the wind-tunnel tests.

References

[1]Rao, D. M., "Leading Edge Vortex-Flap Experiments on a 74 deg. Delta Wing," NASA CR-159161, Nov. 1979.

[2]Marchman, J. F., III, "Effectiveness of Leading-Edge Vortex Flaps on 60- and 75-Degree Delta Wings," *Journal of Aircraft*, Vol. 18, No. 4, 1981, pp. 280–286.

[3]Hoffler, K. D., and Rao, D. M., "An Investigation of the Tabbed Vortex Flap," *Journal of Aircraft*, Vol. 22, No. 6, 1985, pp. 490–497.

[4]Frink, N. T., "Subsonic Wind-Tunnel Measurements of a Slender Wing–Body Configuration Employing a Vortex Flap," NASA TM-89101, July 1987.

[5]Rinoie, K., and Stollery, J. L., "Experimental Studies of Vortex Flaps and Vortex Plates," *Journal of Aircraft*, Vol. 31, No. 2, 1994, pp. 322–329.

[6]Levin, D., and Seigner, A., "Experimental Investigation of Vortex Flaps on Thick Delta Wings," *Journal of Aircraft*, Vol. 31, No. 4, 1994, pp. 988–991.

[7]Traub, L. W., "Aerodynamic Characteristics of Vortex Flaps on a Double-Delta Planform," *Journal of Aircraft*, Vol. 32, No. 2, 1995, pp. 449, 450.

[8]Deng, Q., and Gursul, I., "Effect of Leading-Edge Flaps on Vortices and Vortex Breakdown," *Journal of Aircraft*, Vol. 33, No. 6, 1996, pp. 1079–1086.

[9]Rinoie, K., Fujita, T., Iwasaki, A., and Fujieda, H., "Experimental Studies of a 70-Degree Delta Wing with Vortex Flaps," *Journal of Aircraft*, Vol. 34, No. 5, 1997, pp. 600–605.

[10]Jones, R., Miles, J. W., and Pusey, P. S., "Experiments in the Compressed Air Tunnel on Swept-back Wings Including Two Delta Wings," Aeronautical Research Council Reports and Memoranda 2871, London, 1954.

[11]Fletcher, H. S., "Low-Speed Experimental Determination of the Effects of Leading-Edge Radius and Profile Thickness on Static and Oscillatory Lateral Stability Derivatives for a Delta Wing," NACA TN-4341, July 1958.

[12]Henderson, W. P., "Effects of Wing Leading-Edge Radius and Reynolds Number on Longitudinal Aerodynamic Characteristics of Highly Swept Wing–Body Configurations at Subsonic Speeds," NACA TN D-8361, Dec. 1976.

[13]Chu, J., and Luckring, M., "Experimental Surface Pressure Data Obtained on 65° Delta Wing Across Reynolds Number and Mach Number Ranges," NASA TM 4645, Feb. 1996.

[14]Hu, B. K., and Stollery, J. L., "The Performance of 60° Delta Wings: The Effects of Leading Edge Radius and Vortex Flaps," College of Aeronautics Rept. No.9004, Cranfield Inst. of Technology, Bedford, England, U.K., March 1990.

[15]Rinoie, K., "Low Speed Aerodynamic Characteristics of 60° Rounded Leading-Edge Delta Wing with Vortex Flaps: Part 1. 457.2mm Span Delta Wing," College of Aeronautics Rept. 9611, Cranfield Univ., Bedford, England, U.K., Dec. 1996.

[16]Wentz, W. H., Jr., and Kohlman, D. L., "Vortex Breakdown on Slender Sharp-Edged Wings," *Journal of Aircraft*, Vol. 8, No. 3, 1971, pp. 156–161.

[17]Traub, L. W., "Comparative Study of Delta Wings with Blunt Leading Edges and Vortex Flaps," *Journal of Aircraft*, Vol. 33, No. 4, 1996, pp. 828–830.

[18]Rao, D. M., and Campbell, J. F., "Vortical Flow Management Techniques," *Progress in Aerospace Sciences*, Vol. 24, 1987, pp. 173–224.